The Trifluoromethoxy Carbonyl Peroxy Radical $CF_3OC(O)OO$

Stefan von Ahsen,[a] Helge Willner,*[a] and Joseph S. Francisco[b]

Abstract: $CF_3OC(O)OO$ radicals are generated by low-pressure flash thermolysis of $CF_3OC(O)OOOC(O)OCF_3$ highly diluted in inert gases and followed by subsequent isolation in an inert-gas matrix at low temperatures. The by-products CO_2, COF_2, CF_3O, and CF_3OO are detected. The new peroxy radical is characterized by IR and UV spectroscopy and by its UV photolytic decay which leads to the formation of CF_3OO and CO_2. According to DFT calculations the existence of three stable rotamers is predicted and two of them are found experimentally.

Keywords: density functional calculations • IR spectroscopy • matrix isolation • peroxy radicals • UV/Vis spectroscopy

Introduction

Peroxy radicals formed by atmospheric degradation of chlorofluorocarbons (CFCs) or their alternatives (hydrogen-containing polyhalogenated alkanes or ethers) are relatively stable intermediates.[1] The major constituents of the atmosphere do not react with such radicals, but fast reactions occur with trace gas species like CO, NO, NO_2, or HOO. Although the influence of the peroxy radicals on the atmospheric ozone concentration is seen as negligible today,[2] these radicals have other effects on air pollution or climate. For example, peroxy radicals easily form peroxy nitrates,[3] which serve as reservoir species for nitrogen dioxide. In addition, a potential sink of some fluorinated peroxy radicals is trifluoro acetic acid, a compound for which no biological degradation pathway is known.[4]

An overview of the initial steps of the degradation process of halogenated hydrocarbons is given by Atkinson,[5] and the chemistry of alternative halocarbons and their associated peroxy radicals is reviewed by Francisco and Maricq.[1]

CF_3OO and FC(O)OO are the most basic fluorinated carboperoxy radicals. The IR[6–10] and UV[11, 12] spectroscopic properties of CF_3OO are well documented, as well as several kinetic studies.[11–17] The radical FC(O)OO is less well studied, the IR[10] and UV[10, 18, 19] spectra and some kinetic data[18, 19] are known. While the related species $CF_3C(O)OO$ is partly characterized,[20, 21] to our knowledge no data are available for $CF_3OC(O)OO$. The peroxy radical $CF_3OC(O)OO$ is postulated in studies of the atmospheric degradation of CF_3OCH_3,[22, 23] which leads first to $CF_3OC(O)H$ [see Eqs. (1)–(3)]:

$$CF_3OCH_3 + X + O_2 + M \rightarrow CF_3OCH_2OO + HX + M \ (X = OH, Cl) \quad (1)$$

$$CF_3OCH_2OO + NO \rightarrow CF_3OCH_2O + NO_2 \quad (2)$$

$$CF_3OCH_2O + O_2 \rightarrow CF_3OC(O)H + HOO \quad (3)$$

The trifluoromethyl formate can also be attacked by Cl atoms or OH radicals with subsequent addition of molecular oxygen as seen in Equations (4) and (5):[22, 23]

$$CF_3OC(O)H + X \rightarrow CF_3OCO + HX \ (X = OH, Cl) \quad (4)$$

$$CF_3OCO + O_2 + M \rightarrow CF_3OC(O)OO + M \quad (5)$$

This mechanism is also supported by the formation of $CF_3OC(O)OONO_2$ in the presence of NO_2.[22] Under laboratory conditions, the catalytic oxidation of CO to CO_2 in the presence of trifluoroacetic acid anhydride (as source for CF_3 radicals), oxygen, and UV light has been studied.[24–26] Recently, in the course of these studies the new trioxide $CF_3OC(O)OOOC(O)OCF_3$ has been isolated and characterized.[27] The modified synthesis of $CF_3OC(O)OOC(O)OCF_3$,[26] at −40 °C instead of 0 °C yields the corresponding trioxide $CF_3OC(O)OOOC(O)OCF_3$ as main product.[27] The proposed scheme[26, 28] for this reaction includes the radicals CF_3OCO and $CF_3OC(O)OO$. The former species CF_3OCO was the subject of a recent matrix isolation study,[28] which is now extended in this paper to the elusive $CF_3OC(O)OO$ radical.

---

[a] Prof. Dr. H. Willner, Dipl. Chem. S. von Ahsen
Fakultät 4, Anorganische Chemie
Gerhard Mercator Universität Duisburg
Lotharstr. 1, 47048 Duisburg (Germany)
Fax: (+49) 203-379-2231
E-mail: willner@uni-duisburg.de

[b] Prof. Dr. J. S. Francisco
Department of Chemistry, Earth and Atmospheric Sciences
Purdue University, 1393 H.C. Brown Building
West Lafayette 47907, Indiana (USA)
E-mail: francisc@purdue.edu

Results and Discussion

Low-pressure flash thermolysis of $CF_3OC(O)OOOC(O)OCF_3$ in an excess of Ar or Ne and subsequent quenching of the reaction-gas mixture as a noble-gas matrix at low temperatures results, according to IR spectroscopy, in the formation of a new compound. As no direct structure analysis like X-ray diffraction is available to identify this compound an identification is only possible by the use of absorption spectroscopy and by studying further reactions of the matrix-isolated species. The observation and spectroscopic identification of secondary decomposition products of the unknown species under controlled conditions gives reliable information on the formula, structure, and connectivity of the new molecule. Therefore we present first the results of the “chemical analysis” performed by photolysis experiments of the matrix-isolated thermolysis products of $CF_3OC(O)OOOC(O)OCF_3$ and by changing the thermolysis conditions. After the identification of the new compound as $CF_3OC(O)OO$ a spectroscopic characterization of this compound follows.

Formation and identification of $CF_3OC(O)OO$: When treating the trioxide $CF_3OC(O)OOOC(O)OCF_3$ by a low-pressure flash thermolysis with subsequent quenching of the reaction products in a Ne or Ar matrix at 6 or 16 K, respectively, the trioxide does not survive temperatures of the spray on nozzle above 160 °C. Because in the heated zone the partial pressure of the trioxide is about 10^{-3} mbar and the residence time of the trioxide/noble gas mixtures is about 10^{-3} s, mainly monomolecular reactions occur and the weakest bond is broken according to Equation (6) [reaction enthalpy of the reaction in Eq. (6) amounts 65.1 kJ mol^{-1}, calculated with B3LYP method and 6-311G(d,p) basis set]:

$$CF_3OC(O)OOOC(O)OCF_3 \xrightarrow{\Delta} CF_3OC(O)OO + [CF_3OCO_2] \tag{6}$$

Besides several new IR bands, the carboxyl radical, CF_3OCO_2, is not detected in the matrix IR spectra because it is very weakly bound and secondary dissociation occurs [Eq. (7)]:

$$[CF_3OCO_2] \rightarrow CF_3O + CO_2 \tag{7}$$

The trifluoromethoxy radical[29] and CO_2 are identified by their known IR spectra and, in addition, a small amount of COF_2 is found. To evaluate which species can be attributed to the new IR bands, two further experiments were performed. 1) The pyrolysis temperature was increased in order to follow the thermal decomposition of the new species. At nozzle temperatures above 240 °C the intensities of the new bands decreased and at 300 °C only CO_2, COF_2, CO, and OF together with an increased amount of CF_3O were found. 2) The pyrolysis products of $CF_3OC(O)OOOC(O)OCF_3$ at 160 °C were irradiated with UV light of a mercury high-pressure lamp in combination with a cut off filter (280 nm) or an interference filter ($\lambda = 254$ nm). All unidentified IR bands disappeared simultaneously, while the bands of CF_3O showed a slower decay due to its comparable small absorption cross sections for the light used.[29] CF_3OO[6, 10] was identified as a photolysis product, together with CO_2 and COF_2. When using UV light with wavelength shorter than 254 nm, the photochemically generated CF_3OO is also partially photolyzed. The results can be rationalized by the following reactions [Eqs. (8)–(10)]:

$$CF_3OC(O)OO \xrightarrow{\Delta} COF_2 + CO_2 + OF \tag{8}$$

$$CF_3O{-}C(O)OO + h\nu \rightarrow CF_3O{-}O + CO_2 \tag{9}$$

$$CF_3OC(O)OO + h\nu \rightarrow [CF_3OCO_2 + O] \tag{9a}$$

$$[CF_3OCO_2 + O] \rightarrow [CF_3O + CO_2 + O] \tag{9b}$$

$$[CF_3O + CO_2 + O] \rightarrow CF_3OO + CO_2 \tag{9c}$$

$$CF_3O + h\nu \rightarrow COF_2 + F \tag{10}$$

Equation (8) describes the thermal decay of $CF_3OC(O)OO$ at higher spray on nozzle temperatures. The photolytic dissociation of the trifluoromethoxy carbonyl peroxy radical shown in Equations (9a)–(9c) occurs in the matrix cage. In the first step the excitation of the radical with UV light leads to the dissociation and formation of an oxygen atom trapped in the same matrix cage simultaneously with the carboxyl radical. The carboxyl radical also dissociates yielding carbon dioxide and the trifluoromethoxy radical. The final step is the recombination of CF_3O with the oxygen atom.

The new IR absorber in the thermolysis products of $CF_3OC(O)OOOC(O)OCF_3$ can now be attributed to the $CF_3OC(O)OO$ radical. At higher nozzle temperatures up to 300 °C no CF_3OCO was found. This indicates a strong $CF_3OC(O){-}OO$ bond. Assuming a similarity between the CF_3O group and a fluorine atom, the $CF_3OC(O)OO$ radical should behave similar to FC(O)OO. Indeed, comparable properties were observed in certain cases:

1) The O_2 moiety is strongly bound to carbon and can only be abstracted by raising the pyrolysis temperature (>500 °C in the case of FC(O)OO[10] and 300 °C in the case of $CF_3OC(O)OO$ as discussed above).
2) The generation of the peroxy radical from the trioxide precursors FC(O)OOOC(O)F[10, 30] or $CF_3OC(O)OOOC$-keo(O)OCF_3[27] is possible by low-pressure flash thermolysis in high yields.
3) The photolytic decays according to Equations (9) and (11)[10] are similar:

$$F{-}C(O)OO + h\nu \rightarrow F{-}O + CO_2 \tag{11}$$

Nevertheless, the generation of $CF_3OC(O)OO$ from codeposition matrix-isolation experiments of CF_3O radicals with CO/O_2 mixtures according to Equations (12) and (13) failed. The only observed product was the adduct $CF_3O \cdot O_2$, which is subject of a further study.[31] This result indicates a reaction between CF_3O and O_2 that is much faster than the reaction of CF_3O with CO. In the gas phase under laboratory or atmospheric conditions CF_3OCO should have similar behavior to FCO radicals, which add molecular oxygen rapidly.[1, 18, 19]

$$CF_3O + CO\ (+\ M) \rightarrow CF_3OCO\ (+\ M) \tag{12}$$

$$CF_3OCO + O_2\ (+\ M) \rightarrow CF_3OC(O)OO\ (+\ M) \tag{13}$$

Calculations: All calculations were performed with the Gaussian 98 software package[32] by using density functional theory (DFT).[33] The molecular geometries were first optimized to standard convergence criteria by using the DFT hybrid method with Becke's nonlocal three-parameter exchange,[34, 35] the Lee, Yang, and Parr correction[36] (B3LYP), and a 6-311G(d,p) basis set. As the three dihedral angles are independent, one would expect eight rotamers of $CF_3OC(O)OO$, starting with *trans,trans,trans* $CF_3OC(O)OO$; this implies that the dihedral angles of F-C-O-C, C-O-C-O, and O-C-O-O are 180° (*trans*) and that they change independently of each other to 0° (*cis*). Full optimizations along with vibrational frequency analysis revealed that only three of the eight rotamers are local minima, leading to the rotamers *trans,trans,trans*, or *trans,trans,cis*, or *trans,cis,trans* $CF_3OC(O)OO$, while the other possible isomers have at least one imaginary vibrational frequency. The all-*trans* rotamer is most stable, the *trans,trans,cis* form is higher in energy (ΔH) by 4.7 kJ mol^{-1} and the *trans,cis,trans* isomer by 12.1 kJ mol^{-1}. All given enthalpy values are calculated for standard conditions. The calculated structures of the three stable rotamers of $CF_3OC(O)OO$ are shown in Figure 1.

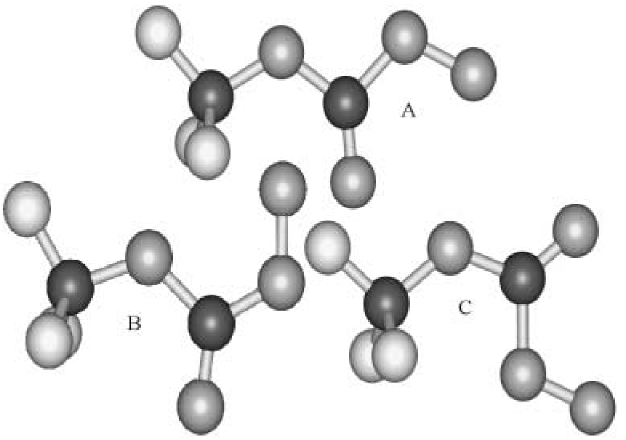

Figure 1. Calculated [B3LYP/6–311G(d,p)] structures of three most stable $CF_3OC(O)OO$ rotamers. A) *trans,trans,trans*-$CF_3OC(O)OO$, B) *trans,trans,cis*-$CF_3OC(O)OO$, and C) *trans,cis,trans*-$CF_3OC(O)OO$.

The *trans,trans,trans* isomer has a C-O-C angle of 118.2°, an O-C-O angle of 102.9°, and a C-O-O angle of 111.8°. The *trans,trans,cis* rotamer has a C-O-C angle of 118.0°, an O-C-O angle of 110.7°, and a C-O-O angle of 116.2°, while the last isomer in *trans,cis,trans* conformation gives values of 125.1°, 109.5°, and 112.5°, respectively. Further molecular properties are collected in Table 1.

Vibrational spectrum: A typical difference IR spectrum of the thermolysis products of $CF_3OC(O)OOOC(O)OCF_3$ isolated in a Ne matrix before and after UV photolysis is shown in Figure 2. The bands of the new species point upwards and those of the photolysis products downwards. The observed IR absorptions are gathered in Table 2.

Table 1. Calculated properties of $CF_3OC(O)OO$[a] rotamers.

		trans,trans,trans	*trans,trans,cis*	*trans,cis,trans*
ΔH [kJ mol^{-1}]		0.0	4.7	12.1
ΔH_R (CF_3OCO[b] + O_2 $\rightarrow CF_3OC(O)OO$)		– 114.5	– 109.8	– 102.4
spin density on	O^a	0.79	0.78	0.80
	O^b	0.18	0.19	0.18
Mulliken charge [e] on	O^a	– 0.07	– 0.08	– 0.05
	O^b	– 0.13	– 0.12	– 0.16
	C^c	0.54	0.54	0.54
	O^d	– 0.25	– 0.26	– 0.23
	O^e	– 0.30	– 0.29	– 0.30
bond length [Å]	O^a–O^b	1.325	1.328	1.324
	O^b–C^c	1.411	1.406	1.416
	C^c–O^d	1.175	1.180	1.173
	O^e–C^c	1.356	1.349	1.356
	C^f–O^e	1.393	1.395	1.392
	avg. C–F	1.327	1.327	1.328

[a] Atom labeling $CF_3O^eC^c(O^d)O^bO^a$. [b] *trans,trans*-CF_3OCO.

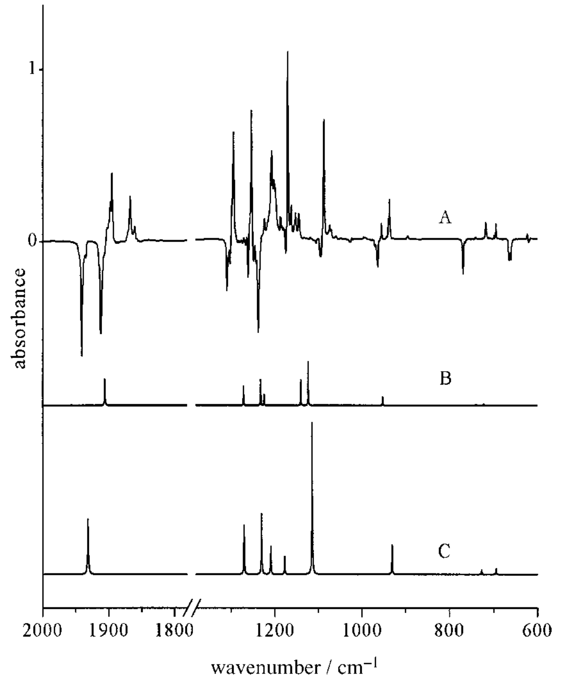

Figure 2. Comparison of experimental and calculated spectra. The upper trace A shows the difference IR spectrum of the pyrolysis products of $CF_3OC(O)OOOC(O)OCF_3$ isolated in Ne matrix before and after UV irradiation. Trace B represents the simulated IR spectrum of *trans,trans,cis*-$CF_3OC(O)OO$, and trace C shows the simulated IR spectrum of *trans,trans,trans*-$CF_3OC(O)OO$ in the estimated molar ratio of rotamer *trans,trans,trans* and *trans,trans,cis* of 4:1.

Assuming C_S symmetry for all rotamers of $CF_3OC(O)OO$, the 18 fundamentals are distributed according to the irreducible representation [Eq. (14)]:

$$\Gamma_{vib} = 12\,A' \text{ (IR, Ra p)} + 6\,A'' \text{ (IR, Ra dp)} \qquad (14)$$

Comparing the experimental IR spectrum with the calculated vibrational data, twelve fundamentals of *trans,trans,trans* $CF_3OC(O)OO$ (given in Table 3) and ten fundamentals of

Table 2. Observed vibrational modes of *trans,trans,trans*- and *trans,trans,cis*-$CF_3OC(O)OO$ isolated in noble gas matrices.[a]

Ne	Ar	Ar	Assignment		Ne	Ar	Ar	Assignment	
$\tilde{\nu}$ [cm^{-1}]	$\tilde{\nu}$ [cm^{-1}]	rel. Int.[b]	*ttt*	*ttc*	$\tilde{\nu}$ [cm^{-1}]	$\tilde{\nu}$ [cm^{-1}]	rel. Int.[b]	*ttt*	*ttc*
25804	2579	0.5	$2\nu_2$		1192	1186	3.8		
2382	2379	0.2	$\nu_3+\nu_5$		1174	1170	75	ν_4	
2064	2062	0.5	$\nu_4+\nu_7$		1167	1162 sh			ν_4
1907	1903	2.6	$\nu_3+\nu_9$		1089	1087	59	ν_5	ν_5
1903	1895	62	ν_1		955	955	6.0		ν_6
1899*	1898*		ν_1		938	936	24	ν_6	
1875	1868	40		ν_1	894	895	2.0	ν_7	
1865*	1861*			ν_1	740	740	1.2	ν_8	ν_8
1298	1295	100	ν_2	ν_2	720	717	10	ν_{16}	ν_{16}
1259	1254	81	ν_{15}	ν_{15}	697	694	7.7	ν_9	
1228	1223	7.8		ν_3		544	0.7		ν_{10}
1206	1207	35	ν_3			401	1.5	ν_{11}	

[a] Band position at the most intensive matrix site, modes marked with an asterisk indicate less intensive matrix sites. [b] Relative integrated band intensities, the strongest observed band ν_2 of both rotamers, is set to 100.

trans,trans,cis $CF_3OC(O)OO$ (presented in Table 4) are identified. Due to similar masses of all atoms and comparable bond strengths all modes are strongly mixed, except for the C=O stretching modes. The approximate descriptions of modes in terms of the dominant coordinate(s) are given in Tables 3 and 4.

In the carbonyl stretching region there are two IR bands in both the Ne and Ar matrices, each occurring as a doublet due to matrix site effects. These bands are assigned to ν_1 of the all-*trans* isomer at 1895 cm^{-1} and of the *trans,trans,cis* rotamer at 1868 cm^{-1} (Ar matrix). The assignment of the stronger band to the *trans,trans,trans* $CF_3OC(O)OO$ is based on the calculations that predict only a slightly higher IR intensity for the C=O stretching mode of the *trans,trans,cis* isomer. Because the intensities of ν_1 of both isomers are calculated to be nearly identical, the experimental ratio of the ν_1 absorption bands mirrors the molar ratio of the two peroxy radicals. Hence a fourfold excess of the all-*trans* form must be present. From the calculations, the third isomer is expected to be present only in traces. The detection limit in our matrix IR spectra is in the range of 5% relative to the main absorber—therefore no band of the third isomer was found.

In the region between 1300 and 850 cm^{-1} for each rotamer, seven stretching modes are expected, but only nine of these 14 absorptions could be detected. From the calculations, it is predicted that ν_2, ν_5, and ν_{15} in the two most stable isomers have nearly identical wavenumbers and should therefore overlap in the measured IR spectrum. Nevertheless, the existence of two rotamers is evident from the significantly more intensive overlapping bands than one could expect from the calculations for the all-*trans* $CF_3OC(O)OO$ only. Hence, the absorptions at 1295, 1254, and 1087 cm^{-1} are assigned to both *trans,trans,trans* and *trans,trans,cis* $CF_3OC(O)OO$. Theory predicts a clear separation of ν_3, ν_4, ν_6, and ν_7 of each rotamer. Considering the calculated intensities and energy difference between *trans,trans,trans* and *trans,trans,cis* $CF_3OC(O)OO$, the fundamentals of the all-*trans* rotamer

Table 3. Experimental and calculated fundamental modes of *trans,trans,-trans*-$CF_3OC(O)OO$.

Ar matrix		Calcd[a]		Approx. description of mode	
$\tilde{\nu}$ [cm^{-1}]	Int.[b]	$\tilde{\nu}$ [cm^{-1}]	Int.		
1895	62	1945	43	ν_1 A′	ν (C=O)
1295	100*	1286	41	ν_2	ν_a (CF_3)
1207	35	1206	15	ν_3	ν (O–C)
1170	75	1178	37	ν_4	ν (CF_3/C–O)[d]
1087	59*	1115	100[c]	ν_5	ν (O–O)
936	24	935	20	ν_6	ν (C–O_2)
895	1.9	892	0.41	ν_7	ν (CF_3/C–O)[e]
740	1.4*	758	0.43	ν_8	δ (CO_3)
694	7.5	692	4.5	ν_9	δ (CF_3)
		557	0.02	ν_{10}	δ (CF_3)
401	1.4	397	0.34	ν_{11}	δ (CO_3/C-O-O)[e]
		376	0.12	ν_{12}	δ (C-O-O)
		308	0.16	ν_{13}	ρ CF_3
		151	0.14	ν_{14}	δ (CO_3/C-O-O)[d]
1254	81*	1245	49	ν_{15} A″	ν_a (CF_3)
717	10*	723	3.6	ν_{16}	γ (CO_3)
		607	0.09	ν_{17}	δ (CF_3)
		428	0.05	ν_{18}	ρ (CF_3)
		138	0.00	ν_{19}	τ (OOCO)
		82	0.06	ν_{20}	τ (FCOC)
		62	0.00	ν_{21}	τ (COCO)

[a] This work, B3LYP/6–311G(d,p). [b] Relative integrated intensities; values marked with an asterisk are assigned to overlapping bands with the *trans,trans,cis* isomer. [c] Relative intensities; the strongest band has an intensity of 799 km · mol^{-1}. [d] Off phase. [e] In phase.

Table 4. Experimental and calculated fundamental modes of *trans,trans,-cis*-$CF_3OC(O)OO$.

Ar matrix		Calcd[a]		Approx. description of mode	
$\tilde{\nu}$ [cm^{-1}]	Int.[b]	$\tilde{\nu}$ [cm^{-1}]	Int.		
1868	40	1923	44	ν_1 A′	ν (C=O)
1295	100*	1287	37	ν_2	ν_a (CF_3)
1223	8.0	1221	11	ν_3	ν (O–C)
1162	sh.	1144	100[c]	ν_4	ν (CF_3/C–O)[d]
1087	59*	1115	25	ν_5	ν (O–O)
955	6.1	951	14	ν_6	ν (C–O_2)
		882	0.12	ν_7	ν (CF_3/C–O)[e]
740	1.4*	738	1.6	ν_8	δ (CO_3)
		610	0.06	ν_9	δ (CF_3)
544	0.05	548	3.1	ν_{10}	δ (CF_3)
		538	0.23	ν_{11}	δ (CO_3)
		377	0.07	ν_{12}	δ (C-O-O)
		258	0.36	ν_{13}	ρ CF_3
		158	0.07	ν_{14}	δ (COC)
1254	81*	1247	47	ν_{15} A″	ν_a (CF_3)
717	10*	717	3.7	ν_{16}	γ (CO_3)
		608	0.07	ν_{17}	δ_a (CF_3)
		429	0.06	ν_{18}	ρ (CF_3)
		124	0.02	ν_{19}	τ (OOCO)
		102	0.06	ν_{20}	τ (FCOC)
		51	0.01	ν_{21}	τ (COCO)

[a] This work, B3LYP/6–311G(d,p). [b] Relative integrated intensities; values marked with an asterisk are assigned to overlapping bands with the *trans,trans,trans* isomer. [c] Relative intensities; the strongest band has an intensity of 827 km mol^{-1}. [d] Off phase. [e] In phase.

0947-6539/02/0820-4678 $ 20.00+.50/0

can be located at 1207, 1170, 936, and 895 cm^{-1} due to their higher intensity. For the second rotamer ν_3, ν_4, and ν_6 are located at 1223, 1162, and 955 cm^{-1}, respectively. ν_4 is observed as a shoulder in the strong band at 1170 cm^{-1}, while ν_7 is not found.

Electronic spectrum: A typical difference UV spectrum before and after UV irradiation ($\lambda = 254$ nm) of the thermolysis products of $CF_3OC(O)OOOC(O)OCF_3$ isolated in Ne matrix is presented in Figure 3. A nearly Gaussian shaped absorption band with its maximum at 240 nm is observed. Its contour is similar to the fluorinated peroxy radical absorption bands of CF_3OO and FC(O)OO.[10] The transition is therefore assigned to the $2^2A'' \leftarrow X^2A''$ excitation leading to subsequent dissociation of the radical [Eq. (15)]:

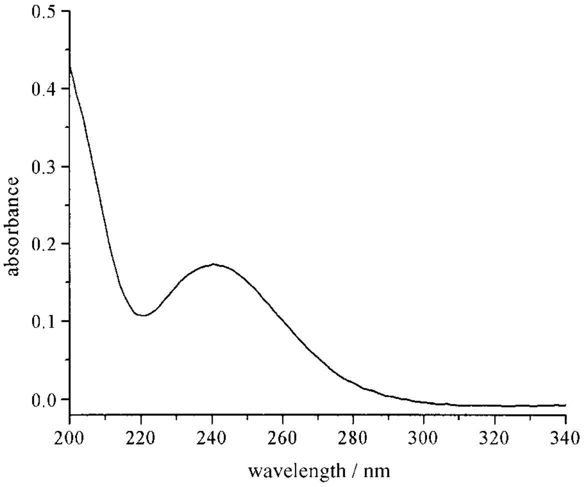

Figure 3. UV spectrum of $CF_3OC(O)OO$ isolated in Ne matrix.

$$CF_3OC(O)OO + h\nu(\lambda = 254\,\text{nm}) \rightarrow [CF_3OCO_2] + O \rightarrow CF_3OO + CO_2 \qquad (15)$$

The photolysis product CF_3OO itself absorbs UV light and this radical partly dissociates during photolysis according to Equation (16).[10]

$$CF_3OO + h\nu(\lambda = 254\,\text{nm}) \rightarrow [CF_3O] + O \rightarrow COF_2 + OF \qquad (16)$$

When using a 225 nm cut-off filter for the photolysis experiment, Equation (16) leads to a complex UV spectrum. The use of UV light with $\lambda = 254$ nm (or longer wavelength) results in CF_3OO as the only UV active photolysis product, which itself is not further affected under the chosen conditions. The also present CF_3O radicals show due to their low-absorption cross section no significant influence on the UV spectra. Therefore no correction to CF_3O was made, while the CF_3OO absorptions, pointing in the direction of negative absorption in the detected difference raw spectra, required a correction. For this purpose, the amount of photochemically generated CF_3OO was derived from the IR difference spectra and the known UV spectrum of CF_3OO[10] was added to the raw spectrum. The final UV spectrum of $CF_3OC(O)OO$ is presented in Figure 3.

In a comprehensive study of fluorinated peroxy radicals, a large similarity in the contour of the $2^2A'' \leftarrow X^2A''$ absorption bands was observed, from which Equation (17), describing the absorption band profile, was taken[1]:

$$\sigma(\lambda) = \sigma_{\max} \exp\{-\alpha[\ln(\lambda/\lambda_{\max})^2]\} \qquad (17)$$

in which σ is the absorption cross section, $\sigma_{\max}$ is the absorption cross section at $\lambda_{\max}$, $\lambda_{\max}$ is the wavelength of the absorption maximum, and α a measure for the width of the Gaussian profile. This profile is a consequence of the Franck–Condon principle for the transition from a bound ground state to a repulsive excited state. As result, for the $2^2A'' \leftarrow X^2A''$ transition of $CF_3OC(O)OO$, the values 240.0($\pm$0.1) nm for $\lambda_{\max}$, and 70.5($\pm$0.7) for α were obtained. We are not able to calibrate the absorbance to absolute absorption cross sections as the formation of $CF_3OC(O)OO$ is not quantitative.

In the ground state X^2A'' of the $CF_3OC(O)OO$ radical, the unpaired electron is mainly located at the terminal oxygen atom of the peroxy moiety in an A''-type orbital. A simplified diagram of the molecular orbitals in peroxy species is given in the literature.[1]

The $2^2A'' \leftarrow X^2A''$ transition is described by an excitation of a π electron from the O_2 unit into a π^*-type orbital. The energy difference between both involved orbitals of A'' symmetry is influenced only by the other A''-type orbitals. Such an influence is expected to be small if the carbon ligand in a radical of the type ROO is CF_3, because the filled A'' orbitals of the fluorine atoms give only a marginal interaction with the OO moiety. In the case of FC(O)OO the carbonyl group possesses a filled and an unoccupied A'' orbital that interact more strongly with the peroxy group. The enlarged number of A'' type orbitals in the energetic region at which the first electronic transitions occur lowers the energetic difference between the involved orbitals. As a consequence the $2^2A'' \leftarrow X^2A''$ transition of FC(O)OO is observed at longer wavelength, as it is found in the case of CF_3OO.[10] By replacing the F atom of FC(O)OO by a CF_3O group, similar properties can be expected. The CF_3O group behaves in several cases as a pseudo-fluorine atom.[28] The Gaussian band profile is found in the UV spectra of the three radicals CF_3OO, FC(O)OO, and $CF_3OC(O)OO$. The red-shift of the absorbance maximum from CF_3OO to FC(O)OO is 26 nm, while it is only 5 nm when going from FC(O)OO to $CF_3OC(O)OO$.

An accurate quantum chemical calculation to simulate the UV spectrum of $CF_3OC(O)OO$ is difficult. The Gaussian98 software package[32] offers the CIS-method[37] to calculate energies for the transition from a molecule's ground state to excited states. The absolute energy values show large deviations from the experimental data, but the described trend in the series CF_3OO, FC(O)OO, and $CF_3OC(O)OO$ is reproduced well by the calculations. While the $2^2A'' \leftarrow X^2A''$ transition for CF_3OO is expected at $\lambda = 156$ nm in its UV spectrum, for FC(O)OO and $CF_3OC(O)OO$ values of 224 nm and 225 nm were obtained as theoretical result, respectively.

At the high-energy limit of the UV spectrum, an additional absorption band is observed as shown in Figure 3. The maximum intensity is slightly below 200 nm, just at the limit of our experimental setup. A computional deconvolution of the UV spectrum locates this maximum of absorbance at 199 nm.

The first electronic excitation—in which one electron is shifted from the highest occupied molecular orbital, offering A′ symmetry, into the semi-occupied orbital—realizes the $1^2A' \leftarrow X^2A''$ transition. This is expected to give an absorption in the near-IR spectral region in accordance with other peroxy radicals like CH_3OO[38] and CF_3OO.[39, 40]

Experimental Section

Caution! The trioxide $CF_3OC(O)OOOC(O)OCF_3$ is potentially explosive, especially in the presence of oxidizable materials. All reactions should be carried out in millimolar quantities only and it is important to take safety precautions when these compounds are handled in the liquid or solid state.

General procedures: Volatile materials were manipulated in glass vacuum lines that were equipped with two capacitance pressure gauges (221 AHS 1000 and 221 AHS 10, MKS Baratron, Burlington, MA), three U-traps used for trap-to-trap condensation, and valves with PTFE stems. The vacuum line was connected to an IR gas cell (20 cm optical path length, Si windows) inside the sample chamber of a FTIR spectrometer (Impact 400 D, Nicolet, Madison, WI). This allowed us to observe the course of reactions and the purification process. $CF_3OC(O)OOOC(O)OCF_3$ was synthesized according to the literature procedure.[27] Ampoules with $CF_3OC(O)OOOC(O)OCF_3$ can be stored in a long term Dewar vessel under liquid nitrogen. By using an ampoule key,[41] the ampoules were opened at the vacuum line, appropriate amounts were taken out for the experiments, and then they were flame-sealed again.

Preparation of the matrices: Small amounts of $CF_3OC(O)OOOC(O)OCF_3$ were transferred in vacuo into a small U-trap immersed in liquid nitrogen. This U-trap was held at −88 °C by an ethanol bath and connected with the heated spray on nozzle in front of the matrix support. A gas stream was directed over the cold sample. For the thermolysis of $CF_3OC(O)OO$-$C(O)OCF_3$ the oven temperature was adjusted to 160 °C. Photolysis experiments on the matrices were undertaken in the UV region using a high pressure mercury lamp (TQ 150, Heraeus, Hanau, Germany) in combination with cut-off or interference filters (Schott, Mainz, Germany). Details of the matrix apparatus are given elsewhere.[42]

Instrumentation: Matrix IR spectra were recorded on a IFS 66 v/S FTIR spectrometer (Bruker, Karlsruhe, Germany) with a resolution of 1 cm^{-1} in the range of 5000 to 400 cm^{-1} in reflectance mode with a transfer optic. A DTGS detector and a KBr beam splitter were used and 64 scans were co-added for each spectrum. Matrix UV spectra were recorded with a Perkin–Elmer Lambda 900 UV/VIS spectrometer (Perkin-Elmer, Norwalk, CT, U.S.) with a resolution of 1 nm (slit 1 nm, integration time 1 s). The spectra were measured in reflectance using two quartz fibres and special condenser optics (Hellma, Jena, Germany).

Acknowledgement

We thank the Deutsche Forschungsgemeinschaft (DFG) and the Fonds der chemischen Industrie for financial support.

---

[1] J. S. Francisco, M. M. Maricq, *Adv. Photochem.* **1995**, *20*, 79.

[2] A. R. Ravishankara, A. A. Turnipseed, N. R. Jensen, S. Barone, M. Mills, C. J. Howard, S. Solomon, *Science* **1994**, *263*, 71.

[3] A. Mayer-Figge, F. Zabel, K. H. Becker, *J. Phys. Chem.* **1996**, *100*, 6587.

[4] M. Emptage, *Biological Degradation of Fluoroacetates*, AFEAS Workshop 2, **1994**.

[5] R. Atkinson, *Atmos. Environ. Part A* **1990**, *24*, 1.

[6] R. Butler, A. Snelson, *J. Phys. Chem.* **1979**, *83*, 3243.

[7] K. C. Clemitshaw, J. R. Sodeau, *J. Phys. Chem.* **1987**, *91*, 3650.

[8] K. C. Clemitshaw, J. R. Sodeau, *J. Phys. Chem.* **1989**, *93*, 3552.

[9] C. Mohua, W. Xuefeng, Y. Min, Q. Qizong, Z. Qike, *Chin. J. Phys. Chem.* **1998**, *11*, 37.

[10] S. Sander, H. Pernice, H. Willner, *Chem. Eur. J.* **2000**, *6*, 3645.

[11] O. J. Nielsen, T. Ellermann, J. Sehested, E. Bartkiewicz, T. J. Wallington, M. D. Hurley, *Int. J. Chem. Kinet.* **1992**, *24*, 1009.

[12] M. M. Maricq, J. J. Szente, *J. Phys. Chem.* **1992**, *96*, 4925.

[13] I. C. Plumb, K. R. Ryan, *Chem. Phys. Lett.* **1982**, *92*, 236.

[14] F. Caralp, R. Lesclaux, M. T. Rayez, J. C. Rayez, W. Frost, *J. Chem. Soc. Faraday Trans.* **1988**, *84*, 569.

[15] J. Peeters, J. Vertommen, I. Langhans, *Ber. Bunsen-Ges.* **1992**, *96*, 431.

[16] J. Sehested, O. J. Nielsen, *Chem. Phys. Lett.* **1993**, *206*, 369.

[17] T. J. Bevilacqua, D. R. Hanson, C. J. Howard, *J. Phys. Chem.* **1993**, *97*, 3750.

[18] M. M. Maricq, J. J. Szente, G. A. Khitrov, J. S. Francisco, *J. Chem. Phys.* **1993**, *98*, 9522.

[19] T. J. Wallington, T. Ellermann, O. J. Nielsen, J. Sehested, *J. Phys. Chem.* **1994**, *98*, 2346.

[20] T. J. Wallington, T. Ellermann, O. J. Nielsen, J. Sehested, *J. Phys. Chem.* **1994**, *98*, 5686.

[21] M. M. Maricq, J. J. Szente, G. A. Khitrov, J. S. Francisco, *J. Phys. Chem.* **1995**, *100*, 4515.

[22] L. K. Christensen, T. J. Wallington, A. Guschin, M. D. Hurley, *J. Phys. Chem. A* **1999**, *103*, 4202.

[23] D. A. Good, M. Kamboures, R. Santiano, J. S. Francisco, *J. Phys. Chem. A* **1999**, *103*, 9230.

[24] M. A. Blesa, P. J. Aymonino, *An. Asoc. Quim. Argent.* **1971**.

[25] F. E. Malanca, G. A. Argüello, E. H. Staricco, *J. Photochem. Photobiol. A* **1997**, *103*, 19.

[26] G. A. Argüello, H. Willner, F. E. Malanca, *Inorg. Chem.* **2000**, *39*, 1195.

[27] S. von Ahsen, P. Garcia, G. A. Argüello, H. Willner, unpublished results.

[28] S. von Ahsen, J. Hufen, H. Willner, J. S. Francisco, *Chem. Eur. J.* **2002**, *8*, 1189.

[29] G. A. Argüello, H. Willner, *J. Phys. Chem. A* **2001**, *105*, 3466.

[30] H. Pernice, M. Berkei, H. Willner, G. Henkel, M. L. McKee, J. D. Webb, unpublished results.

[31] S. von Ahsen, H. Willner, J. S. Francisco, unpublished results.

[32] M. J. Frisch, G. W. Trucks, H. B. Schlegel, G. E. Scuseria, M. A. Robb, J. R. Cheeseman, V. G. Zakrzewski, J. J. A. Montgomery, R. E. Stratmann, J. C. Burant, S. Dapprich, J. M. Millam, A. D. Daniels, K. N. Kudin, M. C. Strain, O. Farkas, J. Tomasi, V. Barone, M. Cossi, R. Cammi, B. Mennucci, C. Pomelli, C. Adamo, S. Clifford, J. Ochterski, G. A. Petersson, P. Y. Ayala, Q. Cui, K. Morokuma, D. K. Malick, A. D. Rabuck, K. Raghavachari, J. B. Foresman, J. Cioslowski, J. V. Ortiz, B. B. Stefanov, G. Liu, A. Liashenko, P. Piskorz, I. Komaromi, R. Gomperts, R. L. Martin, D. J. Fox, T. Keith, M. A. Al-Laham, C. Y. Peng, A. Nanayakkara, C. Gonzalez, M. Challacombe, P. M. W. Gill, B. G. Johnson, W. Chen, M. W. Wong, J. L. Andres, C. Gonzalez, M. Head-Gordon, E. S. Replogle, J. A. Pople, Gaussian 98 (Revision A.5), Gaussian Inc., Pittsburgh PA, **1998**.

[33] W. Kohn, L. J. Sham, *Phys. Rev. A* **1965**, *140*, 1133.

[34] A. D. Becke, *J. Chem. Phys.* **1993**, *98*, 1372.

[35] A. D. Becke, *J. Chem. Phys.* **1993**, *98*, 5648.

[36] C. Lee, W. Yang, R. G. Parr, *Phys. Rev. B* **1988**, *41*, 785.

[37] J. B. Foresman, M. Head-Gordon, J. A. Pople, M. J. Frisch, *J. Phys. Chem.* **1992**, *96*, 135.

[38] H. E. Hunziker, H. R. Wendt, *J. Chem. Phys.* **1976**, *64*, 3488.

[39] S. J. Zalyubovsky, D. B. Wang, T. A. Miller, *Chem. Phys. Lett.* **2001**, *335*, 298.

[40] S. von Ahsen, H. Willner, unpublished results.

[41] W. Gombler, H. Willner, *J. Phys. E: Sci. Instrum.* **1987**, *20*, 1286.

[42] G. A. Argüello, H. Grothe, M. Kronberg, H. Willner, H. G. Mack, *J. Phys. Chem.* **1995**, *99*, 17525.

Received: May 10, 2002 [F4082]